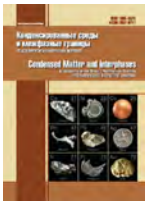

ISSN 1606-867X (Print)
ISSN 2687-0711 (Online)
Condensed Matter and Interphases
Kondensirovannye Sredy i Mezhfaznye Granitsy
https://journals.vsu.ru/kcmf/

Original articles

Research article
https://doi.org/10.17308/kcmf.2021.23/3437

Heat wave dynamics in frozen water droplets with eosin molecules under the femtosecond excitation of a supercontinuum

N. A. Myslitskaya[1,2]✉, A. V. Tcibulnikova[1], I. G. Samusev[1], V. A. Slezhkin[1,2], V. V. Bryukhanov[1]

[1]*Immanuel Kant Baltic Federal University,*
14 A. Nevskogo ul., Kaliningrad 237041, Russian Federation

[2]*Kaliningrad State Technical University,*
1 Sovetsky prospekt, Kaliningrad 237022, Russian Federation

Abstract

In this study, we considered thermal processes in liquid and frozen water droplets with added dye molecules and metal nanoparticles at the moment of supercontinuum generation. We studied optical non-linear processes in a water droplet with a diameter of 1.92 mm, cooled (+2 °C) and frozen to -17 °C, with eosin molecules and ablative silver nanoparticles upon femtosecond laser treatment.

When we exposed a cooled water droplet and a piece of ice containing eosin molecules and ablative silver nanoparticles to a femtosecond laser beam (λ = 1030 nm), we recorded two-photon fluorescence, enhanced by plasmon processes. Also, supercontinuum generation took place, with a period of decay t = 0.02 s. The geometry of non-linear large-scale self-focusing (L_{LSS} ~ 0.45–0.55 mm) was studied. The value of microscale self-focusing (L_{SSS} ~ 0.1 mm) of SC radiation in the laser channel was determined experimentally. The study shows that the energy dissipation in the SC channel increases when the thermal non-linearity exceeds the electronic non-linearity. We modelled the thermal processes and determined the temperature gradient of the heating of the frozen droplet exposed to a femtosecond pulse. Based on the experimental data, the heat wave propagation velocity was calculated to be ν = 0.11 m/s.

Keywords: Supercontinuum, Femtosecond excitation, Water, piece of ice, Eosin fluorescence, Ablative silver nanoparticles, Surface plasmons, Two-photon excitation, Thermal optical non-linearity, Temperature gradient, Heat wave, Wave propagation velocity

For citation: Myslitskaya N. A., Tcibulnikova A. V., Samusev I. G., Slezhkin V. A., Bryukhanov V. V. Heat wave dynamics in frozen water droplets with eosin molecules under the femtosecond excitation of a supercontinuum. *Kondensirovannye sredy i mezhfaznye granitsy = Condensed Matter and Interphases.* 2021;23(2): 260–272. https://doi.org/10.17308/kcmf.2021.23/3437

Для цитирования: Мыслицкая Н. А., Цибульникова А. В., Самусев И. Г., Слежкин В. А., Брюханов В. В. Динамика тепловой волны в сферической замороженной капле воды с молекулами эозина при фемтосекундном возбуждении суперконтинуума. *Конденсированные среды и межфазные границы*. 2021;23(2): 260–272. https://doi.org/10.17308/kcmf.2021.23/3437

✉ Natalia A. Myslitskaya, e-mail: myslitskaya@gmail.com

1. Introduction

For the first time, the phenomenon of the generation of white light in the range of 0.4÷3.0 μm with the formation of a supercontinuum (SC) with a very wide spectrum (low temporal coherence) under femtosecond laser irradiation with an intensity of about ~1 GW/cm^2 was reported in 1970 by Alfano and Shapiro in their works [1].

Spatio-temporal high-intensity localisation of optical energy is accompanied by the non-linear polarisation of the medium and the generation of plasma filaments with the formation of a SC. To date, there have been published significant experimental and theoretical data on the spectral-energy issues of the propagation of a high-intensity electromagnetic field in various media [2–9].

Among the studies of self-focusing laser radiation with SC generation (in the wavelength range of 400–1500 nm) in various media, the most interesting are those in condensed media with silver nanoparticles (SNPs). In such cases, there are changes in the non-linear refractive index due to thermal effects [10–12]. The emergence of a laser pulse track during self-focusing is accompanied by the heating of the medium and a flash of white light, adding Δn to the refractive index due to the heating of the medium. Since the temperature derivative dn/dT can be either positive or negative, both non-linear self-focusing and defocusing can be observed [13, 14].

In this study, we consider thermal processes in liquid and frozen water droplets with eosin molecules and SNPs occurring when a SC is generated upon a femtosecond laser action on the medium. Most of the non-linear refractive index of ice (80–90 %) is associated with electronic polarisation in the optical Kerr effect. However, thermal non-linearity is significant only for nanosecond and longer pulses [15], especially under pulsed femtosecond laser irradiation.

At the same time, thermal non-linearity is an essentially non-local effect due to thermal conduction processes that occur not only in the volume where SC propagates, where radiation is absorbed, but also in neighbouring regions.

In this regard, this article is devoted to the study of the kinetics of thermal processes in the SC channel, when SC is generated in a piece of ice containing eosin and ablative silver nanoparticles.

2. Experimental

We studied water droplets with eosin and SNPs, hanging on a steel needle. In this study, we used SNPs with an average radius of 36 nm, obtained by femtosecond laser ablation of chemically pure silver in bidistilled water. The droplet diameter was 1.92 mm. It was measured using an Olympus BX43 microscope with a video camera. A droplet was cooled from room temperature to –17 °C by blowing it with gaseous nitrogen, obtained by heating liquid nitrogen in a cryostat using a thermoelement. The temperature was measured with a chromel-copel thermocouple, its wires were located inside a microsyringe on which the droplet was hanging. Spectral-energy processes were registered using a linear optical sensor (OOO LOMO FOTONIKA based on Toshiba TCD-1304 linear CCD sensor) with temporal resolution 0.2 ms and spectral resolution 2 nm, and a MotionPro X4 high-speed motion camera (REDLAKE). The study of the SC generation in aqueous solutions was carried out using an Avesta TETA-25 femtosecond laser complex with an ytterbium crystal (pulse parameters: duration τ = 280 fs, energy W = 150 μJ, wave length λ = 1030 nm, pulse repetition frequency ν = 25 kHz, and the duration of a pulse train t_{tr} = 0.2 s).

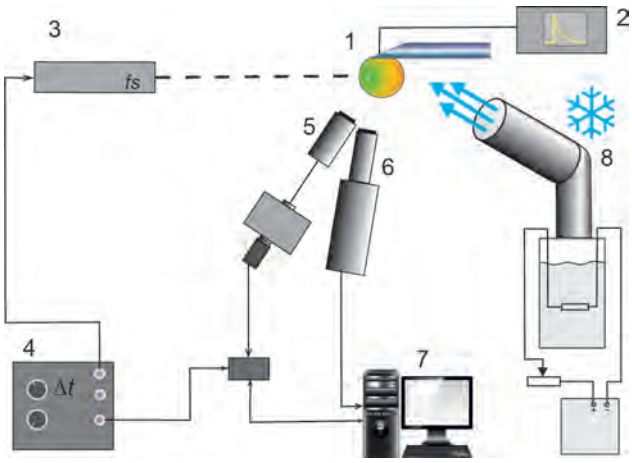

Fig. 1. Layout of the main elements of the laser system: *1* – thermocouple droplet holder; *2* – oscilloscope connected to a thermocouple, *3* – Avesta TETA-25 ytterbium femtosecond laser; *4* – G5-56 double-channel pulse generator; *5* – monochromator with optical linear scale and telescope; *6* – MotionPro X4 high-speed motion camera (by REDLAKE); *7* – computer with specialised signal processing program; *8* – nitrogen gas generator

Droplets of solutions containing eosin molecules and SNPs were frozen to temperature T = –17 °C, then the formed pieces of ice were exposed to a femtosecond pulse train and emission spectra of SC were recorded.

In order to obtain a SC, we used a quartz lens with focal length f = 50 mm for the optical compression of radiation. As a result, filaments were formed inside the water droplet in the SC emission channel with a diameter of less than 100 μm. The power density of the pulse was about $6.8 \cdot 10^{16}$ W/m^2. The SC emission was always excited by a train of femto pulses with a repetition period of 40 μs and a total train duration of t_{tr} = 0.2 s (a total of $5 \cdot 10^3$ pulses in a train).

3. Results and discussion

The study of energy processes accompanying the SC generation in condensed media is mainly aimed at studying liquid aqueous solutions [4, 7], depending on the temperature and the presence of metal nanoparticles and other substances. We wanted to carry out a comparative study of non-linear processes (optical, thermal) taking place upon the SC generation in solutions of eosin with SNPs at temperatures near zero and in frozen solutions. Dye molecules have a high quantum yield, which can be specially enhanced by plasmonic processes in the presence of nanoparticles of precious metals (silver, gold). Therefore, providing that the ingredient concentrations are constant, they can be used for studying SC processes in aqueous and frozen solutions.

In the first set of experiments, we studied the SC generation upon femtosecond laser action on aqueous eosin solutions with a concentration of $C_e = 2 \cdot 10^{-4}$ M with added SNPs with a concentration $C_{Ag} \approx 10^{-12}$ M at low temperature. The excitation power of aqueous solutions with SNPs and dye molecules was < 1.0 MW without compression, the peak power of the pulse significantly exceeded the power threshold of self-focusing in pure distilled water, which is P_c = 0.63 MW [16] ($P_c = c\lambda^2/(32\pi^2 n_2)$, where n_2 is the non-linear refractive index). Under these conditions we managed to obtain the SC emission upon irradiation self-focusing with a power density of about $6.8 \cdot 10^{16}$ W/m^2 [17]. Eosin molecules and SNPs were added to the aqueous solution in order to achieve the plasmon effect on the processes of fluorescence in the solution during the SC generation [18].

Fig. 2a shows one of the video frames of a water droplet with an exposure t_{exp} = 0.002 s at a temperature T = +2.0°C.

The droplet is illuminated for the duration of the excitation laser train t_{tr} = 0.2 s. The laser beam (λ = 1030 nm) incident on the surface of the droplet was focused by a lens. As a result, a bright luminous white spot appeared, with a size of less than 100 μm. The SC generation at this point is due to a change in the refractive index on the spherical surface of the droplet at the air-water interphase. Against the "silhouette" of a spherical water droplet, we can see bright filaments of the SC emission in different areas of the droplet. When the beam entered the water (indicated by the

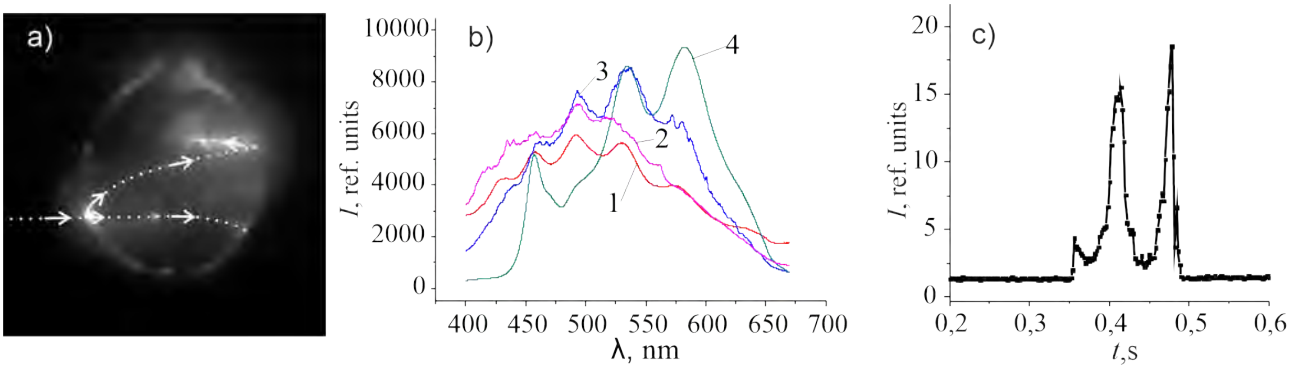

Fig. 2. Video frame of a water droplet with eosin and SNPs (a). The arrows show the propagation of laser radiation after entering the droplet. The SC spectra (b) with an envelope curve with phase modulation of the radiation signal in a water droplet at a temperature of T = 2.0 °C: *1* and *2* – droplets of pure water at different excitation power; *3* and *4* – water droplets containing eosin without SNPs or with SNP, respectively. Change (c) of the integral intensity of the SC emission in a droplet with eosin and SNP during the radiation train lasting for t = 0.2 s

arrow), the emission of water vapour in the form of a mist was recorded. In the upper part of the SC input spot, there was a track of the refracted beam (shown by the arrow), which went in an arc to the upper part of the droplet, where the SC filament appears. According to the laws of refraction, the beam was reflected on the inner water-air interphase and the SC filament was generated, accompanied by flashes of plasma filaments. In the lower part of the SC input spot, the laser beam remained horizontal, it was an extension of the exciting beam (horizontal arrow). In this direction, along the arrow, a bright luminous point inside the droplet was recorded at some distance from the SC spot. Then the beam curved and left the droplet without generating a SC.

Two physical non-linear processes can be considered, when the laser radiation propagates in a cooled droplet at T = +2.0 °C. First, part of the laser light entering the droplet propagates according to the laws of linear optics along a curvilinear track (the upper beam in Fig. 2a). Meanwhile, the power of this radiation decreases and no SC is recorded. However, upon the water-air transition of the beam, the radiation self-focuses additionally at the point of refraction and the SC is generated. It rapidly decays, not reaching the centre of the droplet. Secondly, we have another part of the incoming radiation at the bottom of the SC emission spot (lower part of the figure). In the aqueous medium, a non-linear self-focusing of the infra-red radiation is recorded there at some point along the beam's track, where the eosin fluorescence occurs (λ = 532 nm) under two-photon excitation. This issue will be discussed further when studying the processes of SC generation in a frozen droplet. It should be noted that no such beam splitting processes were recorded in the water droplet at room temperature, only chaotic thin filaments of plasma spark glow and Kerr non-linear polarisation appeared (see article [17]).

Thus, in a water droplet cooled almost to the freezing point, various non-linear processes of light refraction and two-photon excitation of fluorescence of eosin with SNPs occur. When radiation transfers into another medium, SC filamentation takes place.

It is known that filaments of the SC generated by high-intensity laser action are sources of broadband optical radiation with a maximum at the radiation wavelength. Since we studied the generation processes in aqueous solutions containing eosin molecules and SNPs, occurring under intense laser irradiation, it was of interest to obtain information on the spectral composition of the SC in water at a low temperature, T = +2.0 °C.

Figure 2b shows the instantaneous spectra of the SC emission in droplets of pure bidistilled water at a low temperature with broadening due to phase modulation of radiation (Fig. 2b, curves *1* and *2*). It also presents the SC spectra with the emission maxima in water containing eosin molecules without SNPs (Fig. 2b, curve *3*) and with SNPs (Fig. 2b, curve *4*).

The presence of phase modulation in the emission channel with spectral broadening of the SC is accompanied by spectral emission of the constituent elements in samples of different physical natures. When analysing the SC generation spectra, it must be noted that self-focusing is accompanied by an uncontrolled change in the intensity of the laser pulse phase, resulting in the complex spatial dynamics of the laser beam, which is further complicated by the fluctuation of laser radiation [2]. Consequently, the spectrum will exhibit chaotic changes in the intensity of the SC emission along the front edge of the SC emission envelope. Thus, when recording the SC spectra in the 400–700 nm wavelength range, each frame with an exposure of t_{exp} = 0.002 s shows a set of spectral bands of absorption-emission from the components in the SC channel. Thus, by studying the features of the spectral distribution of the SC emission maxima, we can determine the SC spectra of pure water (Fig. 2b, curves *1* and 2). The obtained spectra are well known because they are scientifically valuable references [4].

When the solution contains eosin molecules and SNPs, SC generation is accompanied by the excitation of localised surface plasmons in the SNPs. It is characterised by the scattering-emission spectrum in the wavelength range of 420–460 nm (Fig. 2b, curve *3*) [8,18,19]. Figure 2b, curve *4,* shows the SC spectrum of the eosin solution with SNPs. This spectrum reflects the simultaneous excitation of amplified fluorescence of eosin molecules in the SC channel of a water droplet under the influence of plasmons with

maxima at wavelengths of 530 nm and 580 nm (Fig.2b, curve 4). It also shows the scattering-emission spectrum of the SNP emission in the wavelength range of 420-460 nm [20].

Thus, the instantaneous SC emission spectra of eosin solutions with SNPs near the freezing point (T = +2.0 °C) reflect the processes of SC generation in pure water and the SC spectra of two-photon excitation of fluorescence of eosin molecules, when the fluorescence is amplified by plasmones under the influence of SNPs in a solution.

It should be noted that when studying the spectral features of ultrashort pulses in a condensed medium, the authors showed in article [21] that the spectral dynamics can be simulated. In this case, simulation can be carried out for SC generation processes with ultrashort femtosecond laser pulses only, due to their strong non-linearity, as well as when solitons are formed [22]. Therefore, with longer femtosecond excitations of SC, it is possible to study only the spectral-time evolution of the envelope of the radiation spectrum of a femtosecond pulse [2].

The processes of SC generation in frozen droplets with eosin molecules (C_e = 2·10^{-4} M) and SNPs (C_{Ag} ≈ 10^{-12} M) occur in a completely different way. Fig. 3a shows video frames of the SC radiation in a piece of ice (the frames were recorded every t_{exp} = 0.002 s) until the SC completely decays. It covers a period of the current laboratory time from 0.302 to 0.322 s from the start of the shooting (t_{sc} = 0.02 s).

Let us consider the optical processes of energy conversion in a piece of ice under femtosecond laser excitation. It was shown above that the SC light emission channel is divided into separate glowing elements (pixels). We considered the change in the intensity of the SC pixels along the emission channel (its cross-section area is 7.85·10^{-9} m^2) along the diameter of the piece of ice from the point of time and the coordinate. In addition, we determined the law relating to a decrease in the integral pixel intensity (pixel cross-section intensity) in the SC channel.

Fig. 4a selectively shows 6 intensity profiles of the SC radiation in a piece of ice at different time points of the existence of the SC. Its total duration was t_{sc} = 0.02 s from initiation to complete decay. The total time of action of a laser radiation train on a piece of ice is t_{tr} = 0.2 s.

First, we determined that the maxima of the SC intensity profiles, which initially (frame

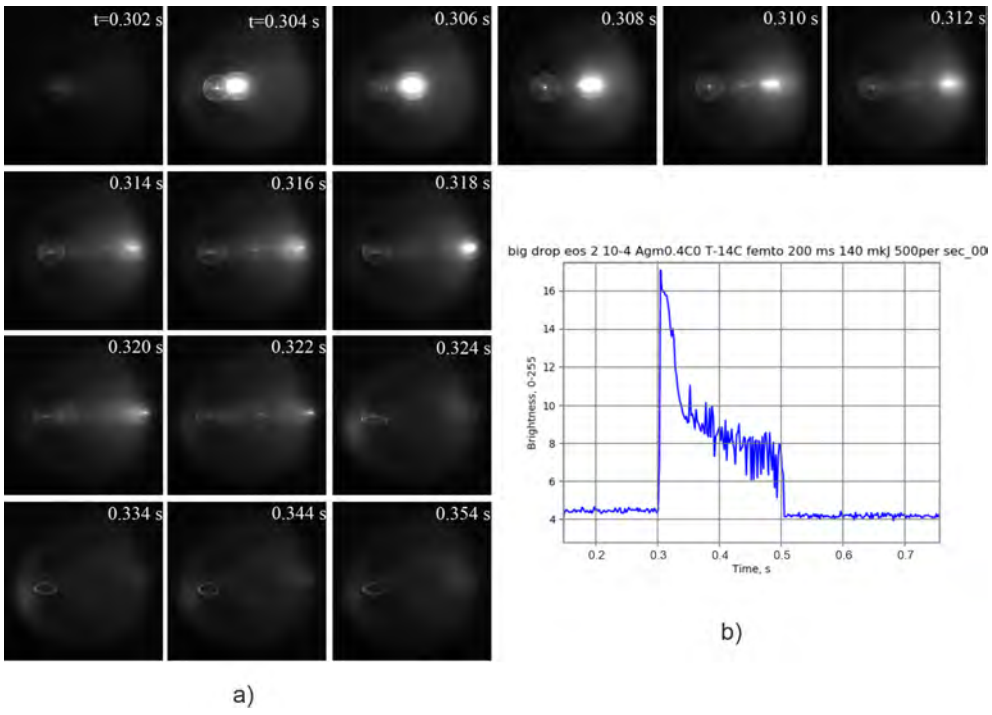

Fig. 3. Video frames (a) of the SC radiation in a frozen spherical droplet at a temperature of –17 °C with eosin molecules and SNPs along the diameter of the frozen droplet, the timestamp of the video shooting is indicated. Kinetic curve of changes in the SC radiation intensity (b)

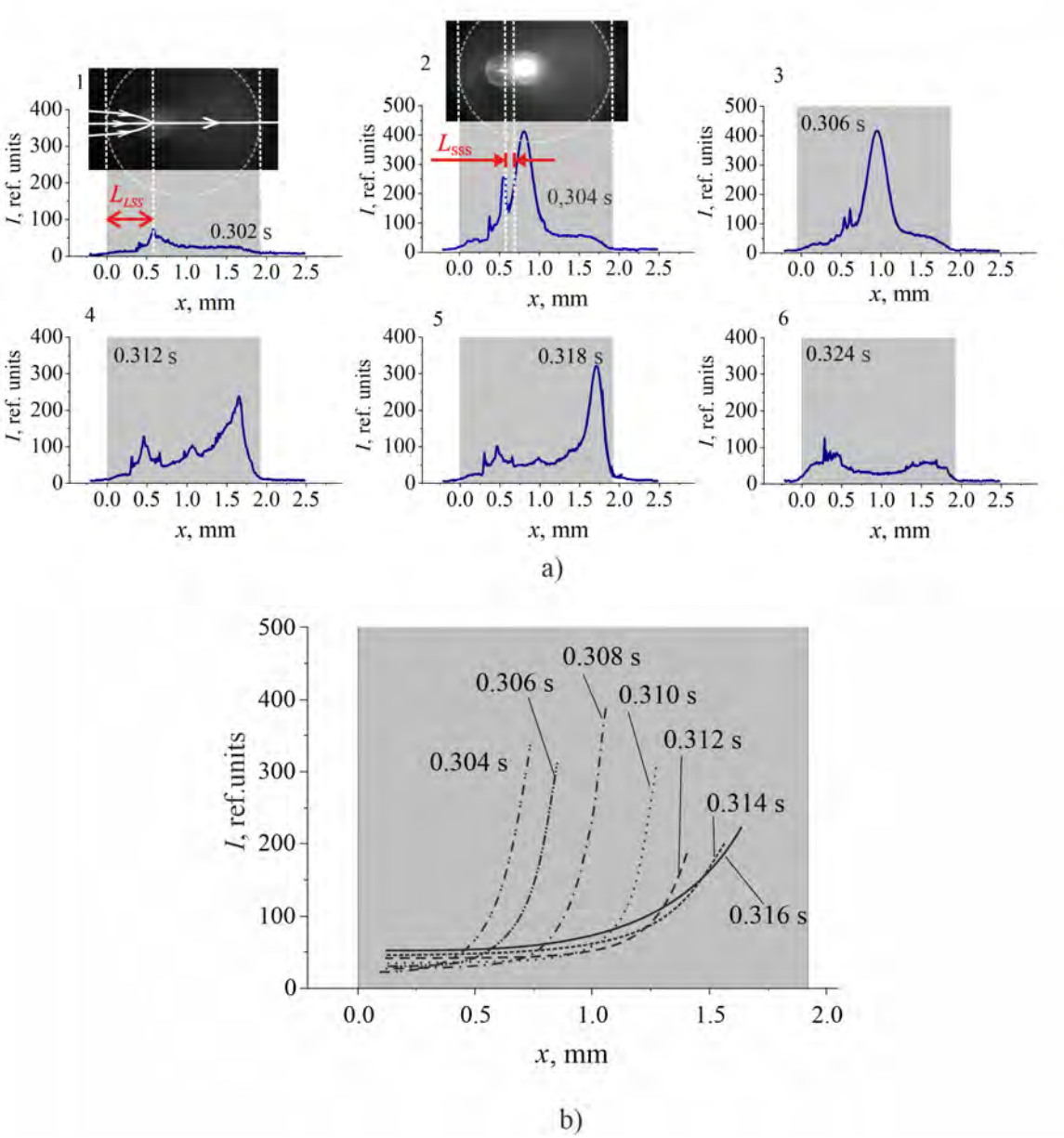

Fig. 4. Profiles (a) of the SC intensity along the diameter of the ice with a time interval of $\Delta\tau$ = 0.002 s (for the frames shown in Fig. 3a). The first profile (1) shows the optical length L_{LSS} of the large-scale focusing of laser radiation entering the piece of ice. The SC intensity profile (2) shows the small-scale focusing distance L_{SSS}. Decay kinetics (b) of the SC radiation fronts along the coordinate along the diameter of the piece of ice

by frame) increased sharply, and then begin to decrease, while moving along the diameter of the piece of ice until the SC completely decays after 0.02 s. The areas of the pixel profiles proportional to the SC intensity were calculated, without taking into account the background light scattering. Then we considered the features of the registered intensities of the SC pixels.

In the first frame (Fig. 4a, profile (1), time point t_1 = 0.302 s), the first pixel in the SC light emission channel was recorded. We can see that the first pixel (1) appears not at the zero coordinate x_0 = 0.0 mm. It is slightly shifted inside the droplet. Obviously, the first SC pixel appears due to the self-focusing of the femtosecond laser beam at a distance of L_{LSS} during the transition from air to the piece of ice. It is followed by Kerr non-linear polarisation of the medium and multiphoton processes [2, 7]. Indeed, when the laser beam passes from air to the piece of ice, non-linear self-focusing of the laser radiation in the ice occurs with the formation of a SC radiation

pixel. Profile (1) in Fig. 4a shows the optical scheme of focusing a laser beam on a spherical surface of a frozen droplet, which is a spot with a linear size of < 100 μm. The scheme is similar to the laser beam focusing on the surface of a cooled drop in Fig. 2; an additional image of the second luminous point of the SC inside the water droplet is also provided. The optical scheme (1) of self-focusing inside a piece of ice presented in Fig. 4a shows the trajectory of the beam in the piece of ice after refraction at a point on the optical axis of the piece of ice.

The appearance of the initial SC emission pixel is associated with the refraction of the laser pulse on the surface of the frozen droplet and its focusing. The focusing is determined by the value of the non-linear index of light refraction in ice:

$$n^* = n_0 + n_2 I_L(t), \quad (1)$$

where n_0 is the reference linear refractive index of ice, n_0 = 1.32; n_2 is the non-linear refractive index, $n_2 = 4.1 \cdot 10^{-16}$ cm^2/W [23]; and $I_L(t)$ is the power density of the radiation incident on the surface of the piece of ice due to the laser pulse compression in air after a focusing lens (see the Experimental section). Using the mathematical model from [4, 24], we determined the focal distance at the so-called critical self-focusing of femtosecond laser radiation after non-linear refraction of radiation in ice by the formula:

$$L_{LSS} = \frac{0.367kr^2}{\left\{\left[\sqrt{\frac{P_0}{P_{cr}}} - 0.852\right]^2 - 0.0219\right\}^{\frac{1}{2}}}, \quad (2)$$

where L_{LSS} is the self-focusing distance on the main optical axis; P_0 is the radiation power; r = 50 μm is the beam radius; and P_{cr} is the critical power of self-focusing. The peak energy in water [4] for a laser pulse with λ = 1032 nm is W =150 μJ, the impulse length is τ = 280 fs. Thus, the peak radiation power is:

$$P_0 = \frac{E}{\tau} = 536 \text{ MW}. \quad (3)$$

The critical radiation power was determined according to Kandidov [4]:

$$P_{cr} = R_{cr} \frac{\lambda^2}{8\pi n_0 n_2} = 2.96 \text{ MW}. \quad (4)$$

Then the distance of self-focusing of radiation and the formation of the focus of the first pixel in ice is L_{LSS} = 0.44 mm.

Considering the SC emission profile (Fig. 4a, profile (1)), it can be seen that the distance between the focus and the surface of the frozen droplet L_{LSS} coincides with the distance of macroscale self-focusing [23, 24] of laser radiation in ice, which is approximately at a distance of 0.44÷0.55 mm from the surface of the droplet. It coincides with the actual position of the first SC radiation pixel. Thus, the experimental values coincide with the modelling parameters for non-linear self-focusing processes. This situation correctly reflects the physical phenomena during SC generation in a spherical piece of ice.

Considering all pixels appearing during the SC generation and decay time t_{sc} = 0.02 s frame by frame, we can see that the first pixel (1) remains still at a distance of 0.44 ÷ 0.55 mm from the surface of the frozen droplet during the entire duration of the SC. Earlier, in [17], a study was carried out of the SC generation at low temperatures with silver NPs in water. It showed that the maximum of SC radiation moves in a medium with the speed of a heat wave. In our study, it was found that, under femtosecond excitation of SC in ice containing eosin molecules (see the Experimental), initially the first immovable SC pixel appears at the self-focusing point L_{LSS}. Moreover, on all profiles (1–6), the coordinate of the first pixel of the SC does not shift and the intensity of this pixel almost does not change.

It was assumed that this fixed pixel of the SC emission recorded in the first frame results from the fluorescence of eosin molecules upon the action of a train of high-intensity femtosecond laser pulses on the piece of ice. Since the laser (ytterbium crystal) radiation occurs at a wavelength of λ = 1030 nm, the molecular fluorescence of eosin molecules (λ_{ex} = 570 nm) could be excited only upon the two-photon excitation of the dye. Thus, in the case of the non-linear self-focusing of a train of laser pulses inside a piece of ice, two-photon fluorescence of eosin molecules with a constant luminous intensity is generated. Since the fluorescence lifetime of eosin molecules is ~ 5 ns, the fluorescence emission remains quasi-continuous under the influence of a train of femtosecond laser pulses.

Fig. 4a, profile (2) shows the profile of SC emission in the piece of ice, obtained by analysing the following video frame, which already includes two SC emission maxima. At the coordinate of 0.4–0.5 mm, there is a complex shaped pixel with a lower intensity, which is visible even on the previous profile. Behind it, at the coordinate ~ 0.66 mm, there is a second pixel. The pixel with a smaller intensity was identified as the maximum of the eosin fluorescence emission upon two-quantum femtosecond laser excitation of the dye. The second, larger maximum on profile (2) indicates a non-linear increase in the perturbation velocity of the SC emission amplitude. Within the limits of this increase, the small-scale perturbations of the refractive index may grow [25]. Considering the intensity development within the second profile (2) at coordinates along the laser channel of the SC x = 0.4÷0.5 mm and x = ~ 0.66 mm, we can use formulas [23–25] to measure the coordinate shift of the amplification of small-scale radiation self-focusing in the SC:

$$\frac{L_{LSS}}{L_{SSS}} \approx \sqrt{\frac{P_0}{P_{cr}}}, \qquad (5)$$

where P_0/P_{cr} is the ratio of the total and critical powers, calculated by formulas (3–4); L_{LSS}/L_{SSS} is the ratio of large-scale and small-scale self-focusing length values. In this case, L_{SSS} ~ 0.033 mm is associated with an increase in the amplitude of non-linear self-focusing upon a change in the refractive index. Analysing the plots (Fig. 4a), we can determine that the experimental value of the small-scale self-focusing is L_{SSS} ~ 0.1 mm, which is ~ 3 times higher than the calculated value of the increase in the SC intensity. It should be noted that the increase in intensity occurs according to a complex dependence, which is indicative of non-linear processes of energy conversion in a piece of ice during the SC generation. For example, Fig. 4b shows the kinetic curves of the growth of the intensity of the front edge of the SC emission in the piece of ice, calculated according to the exponential law, in different temporal coordinates of frame-by-frame recording. It can be seen (Fig. 4b) that the frame-by-frame kinetics of the SC decay in the piece of ice slows down, resulting at the "delay" of the decay time of the SC luminescence after the end of the process. We can assume that the rate of decay of SC in the ice changes because the frozen droplet heats up, which causes a respective change in the refractive index. The resulting thermal non-linearity, as we know from [26], is an essentially non-local effect. Namely, due to heat transfer, the temperature changes not only in the volume absorbing the laser radiation, but also in the neighbouring regions [27–29].

Thus, the studied optical non-linear processes of the kinetics of frame-by-frame decay of the SC radiation in ice samples show a significant effect of thermal processes during focusing and defocusing of radiation inside the SC generation channel. It is known that defocusing occurs in liquids or solids under the conditions of thermal non-linearity, causing a decrease in the refractive index. In this case it is due to the heating of the medium under the action of laser radiation. Approximately 40 μs before the next pulse in the train, the SC energy dissipates in the form of a radial transfer of thermal energy from the volume of the laser channel. It occurs as a result of the decay of the non-linear Kerr polarization (τ ~ 10^{-15}s). During the exposure of each frame, a train of laser radiation consisting of 50 pulses acts on the droplet. The temperature within the excitation channel and around it increases and the refractive index changes. Further, after a period of t_{sc} = 0.02 s, the SC light emission degrades because of the indicated reasons. When the SC in the piece of ice decays, a weakly decaying scattered glow of ice is observed, its intensity almost does not change.

It was of interest to estimate the value of the thermodynamic temperature in the spatio-temporal coordinates of the SC channel, in which the coherent supercontinuum radiation completely degrades. For this purpose, in this work, we measured the areas of all registered SC radiation pixels in the studied samples of frozen droplets frame by frame, using the units of the integral luminous intensity of the pixels.

Fig. 5 shows a graph of the change in the integrated luminous intensity of the SC pixels over the full SC lifetime, t_{sc} = 0.02, approximated by the exponential function

$$I(t) = I_0 + A_1 \cdot \exp\left(\frac{-t - t_1}{t_0}\right), \qquad (6)$$

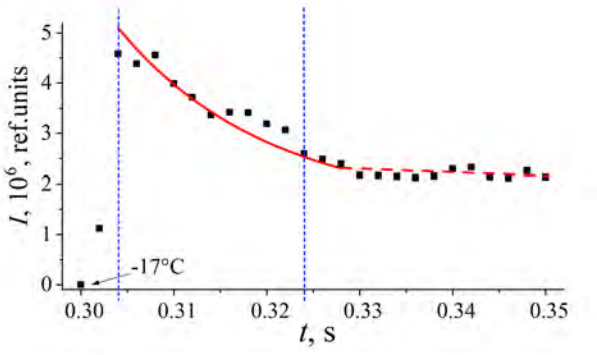

Fig. 5. Decay plot of the integral radiation intensity of the supercontinuum pixels in the frozen droplet with eosin molecules ($C = 2.10^{-4}$ M) and silver nanoparticles ($C_{Ag} \approx 10^{-12}$ M) at an initial temperature of –17 °C. The dashed lines on the time scale indicate the SC generation range

where I_0 is the integral intensity after the decay of the SC filament, background level; A_1 is the maximum increase in SC intensity relative to the background level I_0 at t_1, a moment of time when SC generation begins; t_0 is the average time of the SC decay in the piece of ice after excitation.

When studying the intensity of the SC radiation in the channel along the diameter of the piece of ice at different timepoints of the record, it was found (Fig. 5) that at first the intensity of the SC pixels rapidly increases, reaching a certain maximum, and then exponentially decays according to formula (6). A sharp increase in the SC generation is indicative of the formation of a second radiation pixel (Fig. 4a, profile (2)), which reaches its maximum at a point with a coordinate of approximately ~ 1.0 mm, where non-linear Kerr polarisation arises [2] (at the focusing point of laser radiation). After this, the intensity values of the subsequent pixels of the SC generation decrease over time and shift along the coordinate of the SC radiation channel. The average shifting rate of the shift of the radiation maxima of the SC pixels along the diameter of the piece of ice is $v_1 = 1.92$ mm/0.018 s = 106.6 mm/s ≈ 0.11 m/s.

It should be noted that the spread in the integral values of the intensities of the SC generation pixels (the pixels represent a light guide channel with an ultra-wide spectrum), observed in Fig. 5, is stochastic due to modulation instability in a medium with Kerr-type cubic non-linearity [2, 3]. In this case, possible physical processes causing a decrease in the SC intensity occur as a result of the processes of dissipation of energy obtained during the absorption of radiation in a non-linear medium (electron-phonon interaction, destruction of the anisotropy of the medium in a light field, etc.) and the dissipation of energy with the generation of a heat wave within the SC channel.

Thus, the optical heating of ice resulting from SC generation can cause thermal processes in the SC channel. Their propagation rate is dependent on the temperature gradient and the temperature conductivity index of the medium. As shown above (formula (6)), the decay of the integrated intensity of SC generation in a piece of ice is described by an exponential dependence; simultaneously with this, thermal processes also develop according to the known laws of generation and transfer of heat during laser action [30–32]:

$$C_{(v)} \frac{\partial T}{\partial t} - a\Delta T = \delta \cdot I_L(r). \quad (7)$$

T is the thermodynamic temperature; $C_{(v)} = 1.812 \cdot 10^6$ J/(m^3·K) is the average specific heat of ice at -17 °C; t is the duration of laser radiation; a is the thermal conductivity; δ is the absorption coefficient of ice at the laser radiation wavelength (δ = 10 m^{-1} [33]); and $I_L(r)$ is the intensity of laser radiation in a beam with a radius of r. With a pulsed femtosecond laser action on a piece of ice, we can omit the thermal conductivity a, and, accordingly, the second summand in equation (7), and calculate the instantaneous temperature at the SC generation for a short period of time [21, 23, 34]. In this case, all temperature gradients between molecules and SNPs during the emission period of one SC pixel ($t_{exp} = 0.002$ s) are levelled out due to the fast energy transfer. We can also omit the heat capacity and mass of eosin molecules and SNPs in the generated SC.

Let us calculate the temperature increase on the axis of the piece of ice during the entire time of the action of the train of electromagnetic laser pulse using the following equation, assuming that a stationary temperature field has been established [23]:

$$\Delta T_{fin} = \frac{\delta I r^2}{\kappa}, \quad (8)$$

where δ is the absorption coefficient of ice at the laser wavelength, $\langle I \rangle = W\nu/S = 4.78 \cdot 10^8$ W/m^2 is the average emission power density during the peri-

od of action of the train, S is the section area of the laser beam $S = \pi r^2$, and $\kappa = 2.34$ W/(m·K) is the thermal conductivity index of ice. We found that with $\Delta T_{fin} = 5.1$ K, the temperature on the droplet axis increased to –11.9 °C.

Using the data on the exponential dependence of the SC radiation decay in Fig. 5, assuming that the radiation intensity is proportional to the temperature, and taking into account the obtained data that the initial temperature is –17 °C, and the saturation temperature is –11.9 °C, we can measure the initial sharp increase in the temperature in the channel during 0.002 s, when the temperature reached its maximum value, and more inertial thermal conduction processes have not yet manifested themselves. The maximum intensity value on the graph corresponds to a temperature of –6.0 °C.

We also estimated the temperature at the moment of the maximum intensity of the SC radiation pixel at the coordinate x ~ 0.8 mm from the surface of the frozen droplet. We took into account that heating occurs due to the linear absorption of the radiation energy of 50 laser pulses in the train during $t_{exp} = 0.002$ s. Considering that the distance over which the heat is dissipated by heat transfer can be estimated as $l = (a \cdot t_{exp})^{1/2} \approx 51$ μm [35], the average temperature increase in the channel with a radius $r + l$ amounts to

$$\Delta T_{ch} = \frac{\left(1 - \exp\left(-\delta 2R\right)\right) W \nu t_{exp}}{C_{(v)} \pi \left(r + l\right)^2 2R} \approx 1.3 \text{ °C},$$

but it is important to take into account the uneven distribution of heat in this volume.

We also estimated the average final temperature increment in the entire volume of heated ice after the SC decomposition over the time $t_{sc} = 0.02$ s, which appeared to be only $\Delta T = 0.2$ °C. Therefore, in such work it is necessary to take into account that the temperature field in the volume of the droplet is distributed unevenly. For the indicated time, the SC radiation in the ice completely disappeared as a result of complex physical processes of energy dissipation, such as the decay of non-linear polarization, scattering of optical and thermal energy, etc. One of the indicators of irreversible energy dissipation of the SC in the ice was the registered scattered glow of the ice as a whole, which may be due to the thermal heating of the ice without visible melting upon the action of a train of pulses with a duration of $t_{tr} = 0.2$ s.

Thus, after the first pulse and focusing of the laser beam, as a result of additional refraction on the spherical surface of a frozen water droplet with eosin molecules and SNPs, the SC amplifies with maximum intensity. During the lifetime of the SC radiation in the ice ($t_{sc} = 0.02$ s), the piece of ice in the laser channel heated up from –17 to –11.9 °C.

A temperature gradient in the laser channel with eosin molecules and SNPs upon femtosecond laser photoexcitation of the medium makes it possible to simulate the generation of a thermal wave in a non-linear medium. Namely, we can calculate the propagation velocity of a thermal wave according to the equation [30]:

$$\nu = \sqrt{\frac{\kappa}{C_{(v)} \tau_r}}, \quad (9)$$

where ν is the propagation velocity of a heat wave; $\kappa = 2.34$ W/(m·K) is the thermal conductivity of ice at –17 °C; $C_{(v)} = C\gamma$ is the volumetric heat capacity of ice, where $C = 1.972 \cdot 10^3$ J/(kg·K) is the specific heat capacity of ice; $\gamma = 919$ kg/m^3 is the density of ice; and $\tau_r = 1 \cdot 10^{-5}$ s is the dielectric relaxation time of ice [36]. Calculations show that $\nu \approx 0.359$ m/s.

Thus, before the complete decay of the SC in a laser-heated ice with eosin and SNPs, a thermal wave is generated with a velocity of $\nu = 0.11$ m/s. Its value almost coincides with the theoretical value of the propagation velocity of a thermal wave in ice.

4. Conclusions

In this work, we studied optical non-linear processes in water droplets in liquid and frozen states with eosin molecules and SNPs at the moment of supercontinuum (SC) generation under femtosecond laser action on the medium. We obtained the following results:

1. We directed a train (duration $t_{tr} = 0.2$ s) of femtosecond pulses at a power density of about $6.8 \cdot 10^{16}$ W/m^2 ($\lambda = 1030$ nm) on a spherical water droplet with a temperature of +2.0 °C, containing eosin and SNPs. As a result, we observed a spectrum of coherent SC radiation with phase

modulation and the spectrum of SNP plasmons in the wavelength range 420–460 nm. The generation of surface plasmons on SNPs of the droplet led to an increase in the intensity of two-photon fluorescence of eosin molecules in the SC radiation filaments.

2. The action of a train of laser radiation on a piece of ice with eosin and SNPs at –17 °C led to its self-focusing after crossing the air-ice interphase and the generation of a coherent white light SC. Using a high-speed video camera, the pixels of the SC radiation in the ice were recorded frame-by-frame with a time step of t_{exp} = 0.002 s until the the SC radiation decayed completely, the SC lifetime was t_{sc} = 0.02 s. After that, for a period of t_{tr} = 0.2 s, only the decaying scattered glow of a piece of ice without SC was observed.

3. When analysing the geometry of self-focusing of the first SC pixels we determined the distance of non-linear large-scale self-focusing L_{LSS} ~ 0.44–0.55 mm and the experimental value of the distance of small-scale radiation self-focusing L_{SSS} ~ 0.1 mm. These values indicated a rapid increase in the radiation intensity in the SC channel with the first two pixels. When the excitation pulses were repeated with a black period of t ~ 40 μs, the thermal non-linearity exceeded the electron. It accelerated the energy dissipation in the SC channel. Subsequent frames also showed a temporal exponential delay of the light decay at the SC pixels along the generation channel as a result of thermal conduction processes.

4. When simulating the SC generation process, the exponential law of its decay after exposure to a laser pulse was determined. We also determined the instantaneous maximum temperature when the first pixel of the SC radiation in the piece of ice appeared, which is T_{max} = –6.0 °C. The temperature of ice in the radiation channel after decay of the SC is T ≈ –11.9 °C. Thus, it was found that the piece of ice after exposure to a femtosecond electromagnetic pulse train did not melt.

5. The radiation kinetics of the SC pixels along the diameter of a piece of ice with eosin and SNPs indicates the presence of a temperature gradient. The gradient leads to the generation of a heat wave in a non-linear medium, the propagation velocity of which, according to modelling, is ν ≈ 0.359 m/s. If we compare the velocity value obtained by conceptual modelling and the actual velocity value, we can see that $v_1 \sim v$.

Thus, the obtained results of the study of the femtosecond SC generation in a piece of ice containing eosin and SNPs showed that thermal optical non-linearity appears, develops, and degrades during the lifetime of the SC in ice.

Contribution of the authors

Myslitskaya N. A. – research, experimental data processing, design of figures, calculations, text writing. Tcibulnikova A. V. – research, discussion of results. Slezhkin V. A. – preparation of samples, research, discussion of results, text writing. Samusev I. G. – research concept, research methodology, discussion of results. Bryukhanov V. V. – scientific leadership, research concept, methodology development, review writing, calculations, text writing, final conclusions.

Conflict of interests

The authors declare that they have no known competing financial interests or personal relationships that could have influenced the work reported in this paper.

References

1. Alfano R. R., Shapiro S. L. Emission in the region 4000 to 7000 Å via four-photon coupling in glass. *Phys. Rev. Lett.*1970;24(11): 584–587. https://doi.org/10.1103/PhysRevLett.24.584

2. Zheltikov A. M. Let there be white light: supercontinuum generation by ultrashort laser pulses. *Physics-Uspekhi*. 2006;49(6): 605. http://dx.doi.org/10.1070/PU2006v049n06ABEH005975

3. Couairon A., Mysyrowicz A. Femtosecond filamentation in transparent media. *Physics Reports*. 2007;441(2-4): 47–189. https://doi.org/10.1016/j.physrep.2006.12.005

4. Kandidov V. P., Shlemov S. A. Javlenie filamentacii moshhnyh femtosekundnyh lazernyh impul'sov i ego prakticheskie prilozhenija. [The phenomenon of filamentation of high-power femtosecond laser pulses and its practical applications] In: Panchenko V. Ja. (ed.) *Glubokoe kanalirovanie i filamentacija moshhnogo lazernogo izluchenija v veshhestve* [Deep channeling and filamentation of high-power laser radiation in matter]. Moscow, Interkontakt Nauka Publ.; 2009. p. 185–266. (In Russ.)

5. Chin S. L. *Femtosecond Laser Filamentation*. N.Y.: Springer; 2010. 130 p. https://doi.org/10.1007/978-1-4419-0688-5

6. Chekalin S. V., Kandidov V. P. From self-focusing light beams to femtosecond laser pulse filamen-

tation. *Physics-Uspekhi*. 2013;56(2): 123-140. https://doi.org/10.3367/ufne.0183.201302b.0133

7. Apeksimov D. V., Bukin O. A., Bykova E. E., Gejnc Ju. Je., Golik S. S., Zemljanov Al. A., Zemljanov A. A., Il'in A. A., Kabanov A. M., Matvienko G. G., Oshlakov V. K., Sokolova E. B., Habibullin R. R. Interaction of GW laser pulses with water droplets. *Prikladnaja Fizika*. 2011;6: 13–21. Available at: http://applphys.orion-ir.ru/appl-11/11-6/PF-11-6-13.pdf (In Russ., abstract in Eng.)

8. Kudryashov S. I., Samokhvalov A. A., Ageev E. I., Veiko V. P. Ultrafast broadband nonlinear spectroscopy of a colloidal solution of gold nanoparticles. *JETP Lett.*, 2019;109(5): 298–302. https://doi.org/10.1134/S0021364019050096

9. Hoppius J. S., Maragkaki S., Kanitz A., Gregorcic P., Gurevich E. L. Optimization of femtosecond laser processing in liquids. *Applied Surface Science*. 2019;467–468: 255–260. https://doi.org/10.1016/j.apsusc.2018.10.121

10. Liu W., Kosareva O., Golubtsov I.S., Iwasaki A., Becker A., Kandidov V. P., Chin S. L. Femtosecond laser pulse filamentation versus optical breakdown in H_2O. *Applied Physics B: Lasers and Optics*. 2003;76(3): 215–229. https://doi.org/10.1007/s00340-002-1087-1

11. Driben R., Husakou A., Herrmann J. Supercontinuum generation in aqueous colloids containing silver nanoparticles. *Optics Letters*. 2009;34(14): 2132–2134. https://doi.org/10.1364/OL.34.002132

12. Sutherland R. L. *Handbook of Nonlinear Optics*. 2nd Edition. CRC Press; 2003. p. 337–499. https://doi.org/10.1201/9780203912539

13. Ahmanov S. A., Nikitin S. Ju. *Fizicheskaja optika* [*Physical optics*]. Moscow: Nauka Publ.; 2004. 656 p. (In Russ.)

14. Besprozvannyh V. G., Pervadchuk V. P. *Nelinejnaja optika: ucheb. posobie* [Nonlinear Optics: A Tutorial]. Perm': Perm. gos. tehn. un-ta Publ.; 2011. 200 p. (In Russ.)

15. Zhai S., Huang L., Weng Z., Dai W. Parabolic two-step model and accurate numerical scheme for nanoscale heat conduction induced by ultrashort-pulsed laser heating. *Journal of Computational and Applied Mathematics*. 2020;369: 112591. https://doi.org/10.1016/j.cam.2019.112591

16. Lee Smith W., Liu P., Bloembergen N. Superbroadening in H_2O and D_2O by self-focused picosecond pulses from a YAlG: Nd laser. *Physical Review A*. 1977;15(6): 2396–2403. https://doi.org/10.1103/PhysRevA.15.2396

17. Myslitskaya N. A., Tcibul'nikova A. V., Slezhkin V. A., Samusev I. G., Antipov Ju. N., Derevshhikov V. V. Generation of supercontinuum in filamentation regime in a water droplet containing silver nanoparticles at low temperature. *Optics and spectroscopy*. 2020;128(12): 1954–1962. https://doi.org/10.1134/s0030400x20120978

18. Klimov V. V. *Nanoplazmonika*. Moscow: Fizmatlit Publ.; 2009. 480 p. (In Russ.)

19. Balykin V. I. and Melentiev P. N. Optics and spectroscopy of a single plasmonic nanostructure. *Physics-Uspekhi*. 2018;61(2): 133. https://doi.org/10.3367/UFNe.2017.06.038163

20. Myslitskaya N. A., Slezhkin V. A., Borkunov R. Y., Tsar'kov M. V., Samusev I. G., Bryukhanov V. V. Spectral and temperature dynamics of the processes inside aqueous droplets containing eosine molecules and silver nanoparticles upon laser excitation in the IR and visible Ranges. *Russian Journal of Physical Chemistry A*. 2019;93(8): 1559–1566. https://doi.org/10.1134/S003602441908020X

21. Bespalov V. G., Kozlov S. A., Shpolyanskiy Yu. A., Walmsley I. A. Simplified field wave equations for the non-linear propagation of extremely short light pulses. *Physical Review A*. 2002;66: 013811. https://doi.org/10.1103/PhysRevA.66.013811

22. Rozanov N. N., Vysotina N. V., Shacev A. N., Desjatnikov A. S., Shadrivov I. V., Noskov R. E., Kivshar' Ju. S. Discrete switching and dissipative solutions in the coherently excited nanostructures and metamaterials. *Scientific and Technical Journal of Information Technologies, Mechanics and Optics*. 2012;4(80): 1–12. Available at: https://www.elibrary.ru/item.asp?id=17799659 (In Russ. abstract in Eng.)

23. Sizmin D. V. *Nelinejnaja optika* [Nonlinear optics]. Saratov: SarFTI Publ.; 2015. 146 p. (In Russ.)

24. Marburger J. H. Self-focusing: Theory. *Progress in Quantum Electronics*. 1975;4(1): 35–110. https://doi.org/10.1016/0079-6727(75)90003-8

25. Bespalov V. I., Talanov V. I. O nitevidnoi strukture puchkov sveta v nelineinykh zhidkostyakh [On the filamentous structure of light beams in nonlinear liquids]. *JETP Letters*. 1966;3(12): 307–309. Available at: http://jetpletters.ru/cgi-bin/articles/download.cgi/782/article_12073.pdf (In Russ.)

26. Dmitriev V. G., Tarasov L. V. *Prikladnaja nelinejnaja optika. 2nd ed.* [Applied nonlinear optics]. Moscow: FIZMATLIT Publ.; 2004. 512 p. (In Russ.)

27. Shen Y. R. *The Principles of Nonlinear Optics*. New York: Wiley; 1984. 563 p.

28. Boyd R. W. *Nonlinear optics*. 3rd ed. Boston: Academic Press; 2007. 640 p.

29. Lykov A. V. *Teorija teploprovodnosti* [Heat conduction theory]. Moscow: Vysshaja shkola Publ.; 1966. 592 p. (In Russ.)

30. Tabiryan N. V., Luo W. Soret feedback in thermal diffusion of suspensions. *Physical Review E*. 1998;57(4): 4431–4440. https://doi.org/10.1103/PhysRevE.57.4431

31. Baffou G. Rigneault H. Femtosecond-pulsed optical heating of gold nanoparticles. *Physical Review*

B. 2011;84: 035415-1-13. https://doi.org/10.1103/PhysRevB.84.035415

32. Warren S. G., Brandt R. E. Optical constants of ice from the ultraviolet to the microwave: A revised compilation. *Journal of Geophysical Research*. 2008;113(D14220). https://doi.org/10.1029/2007JD009744

33. Brown A. M., Sundararaman R., Narang P., Goddard III W. A., Atwater H. A. Ab initiophonon coupling and optical response of hot electrons in plasmonic metals. *Physical Review B*. 2016;94(7): 075120-1–075120-10. https://doi.org/10.1103/PhysRevB.94.075120

34. Kuhling H. *Handbook of Physics*. Moscow: Mir Publ.; 1982. 519 p. (in Russ.).

35. Libenson M. N., Jakovlev E. B., Shandybina G. D. *Vzaimodejstvie lazernogo izluchenija s veshhestvom (silovaja optika). Chast' II. Lazernyj nagrev i razrushenie materialov. Uchebnoe posobie* [Interaction of laser radiation with matter (power optics). Part II. Laser heating and destruction of materials. Tutorial]. Vejko V. P. (ed.). Sankt Petersburg: NIU ITMO Publ.; 2014. 181 p. (In Russ.)

36. Johari G. P., Whalley E. he dielectric properties of ice Ih in the range 272–133 K. *The Journal of Chemical Physics*. 1981;75(3): 1333–1340. https://doi.org/10.1063/1.442139

Information about the authors

Natalia A. Myslitskaya, PhD in Physics and Mathematics, senior research fellow at the Research & Education Centre "Fundamental and Applied Photonics. Nanophotonics", Institute of Physical and Mathematical Sciences and Information Technologies, Immanuel Kant Baltic Federal University, Kaliningrad, Russian Federation; Associate Professor at the Department of Physics, Kaliningrad State Technical University, Kaliningrad, Russian Federation; e-mail: myslitskaya@gmail.com. ORCID iD: https://orcid.org/0000-0001-6701-5328.

Anna V. Tcibulnikova, PhD in Physics and Mathematics, senior research fellow at the Research & Education Centre "Fundamental and Applied Photonics. Nanophotonics", Institute of Physical and Mathematical Sciences and Information Technologies, Immanuel Kant Baltic Federal University, Kaliningrad, Russian Federation; e-mail: anna.tsibulnikova@mail.ru. ORCID iD: https://orcid.org/0000-0001-8578-0701.

Vasiliy A. Slezhkin, PhD in Chemistry, senior research fellow at the Research & Education Centre "Fundamental and Applied Photonics. Nanophotonics", Institute of Physical and Mathematical Sciences and Information Technologies, Immanuel Kant Baltic Federal University, Kaliningrad, Russian Federation; Associate Professor at the Department of Chemistry, Kaliningrad State Technical University, Kaliningrad, Russian Federation; e-mail: vslezhkin@mail.ru. ORCID iD: https://orcid.org/0000-0002-2801-7029.

Ilia G. Samusev, PhD in Physics and Mathematics, head of the Research & Education Centre "Fundamental and Applied Photonics. Nanophotonics", Institute of Physical and Mathematical Sciences and Information Technologies, Immanuel Kant Baltic Federal University, Kaliningrad, Russian Federation; e-mail: is.cranz@gmail.com. ORCID iD: https://orcid.org/0000-0001-5026-7510.

Valeriy V. Bryukhanov, DSc in Physics and Mathematics, leading research fellow at the Research & Education Centre "Fundamental and Applied Photonics. Nanophotonics", Institute of Physical and Mathematical Sciences and Information Technologies, Immanuel Kant Baltic Federal University, Kaliningrad, Russian Federation; e-mail: bryukhanov_v.v@mail.ru. ORCID iD: https://orcid.org/0000-0003-4689-7207.

Received 20.11.2020; Approved after reviewing 29.03.2021; Accepted 15.05.2021; Published online 25.06.2021.

Translated by Anastasiia Ananeva
Edited and proofread by Simon Cox